Faraday Discussions

Accepted Manuscript

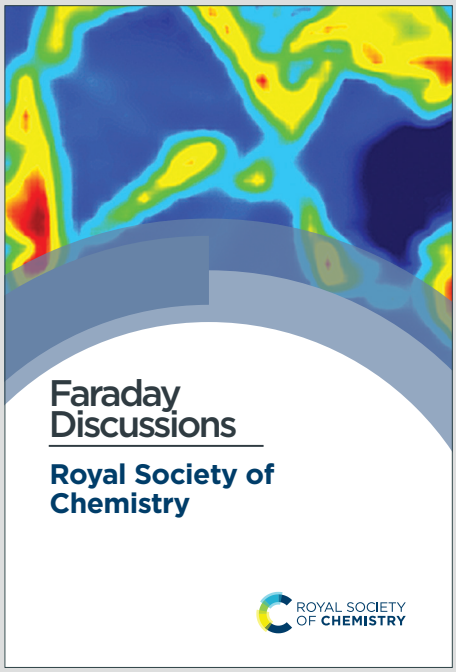

This article can be cited before page numbers have been issued, to do this please use: M. P. Chipperfield, S. Heddell, S. Dhomse, W. Feng, S. Chang, G. Mann, X. Zhou and H. Pumphrey, *Faraday Discuss.*, 2024, DOI: 10.1039/D4FD00163J.

Ongoing large ozone depletion in the polar lower stratospheres: The role of increased water vapour

View Article Online
DOI: 10.1039/D4FD00163J

Martyn P. Chipperfield[1,2], Saffron Heddell[1], Sandip S. Dhomse[1,2], Wuhu Feng[1,3], Shujie Chang[1], Graham Mann[1], Xin Zhou[4], and Hugh Pumphrey[5]

1. School of Earth and Environment, University of Leeds, Leeds LS2 9JT, UK
2. National Centre for Earth Observation, University of Leeds, UK
3. National Centre for Atmospheric Science, University of Leeds, UK
4. School of Atmospheric Sciences, Chengdu University of Information Technology, Chengdu, China
5. School of Geosciences, University of Edinburgh, UK

For submission to Royal Society of Chemistry Faraday Discussion meeting on Atmospheric Chemistry in Cold Environments, Feb 17-19th 2025.

Abstract

The very low temperatures of the polar lower stratosphere lead to the efficient seasonal depletion of ozone following the formation of polar stratospheric clouds (PSCs) and heterogeneous chlorine-activating reactions on their surface. The Montreal Protocol has controlled the production of major chlorine- (and bromine-) containing Ozone Depleting Substances (ODSs) and the stratospheric Cl and Br loadings have been slowly decreasing for over two decades. However, we are still experiencing very large (by some measures record) ozone depletion in the Antarctic and cold Arctic springs. There are a variety of factors involved but here we focus on the possible role of increased stratospheric water vapour, for example as occurred due to the eruption of the underwater volcano Hunga Tonga-Hunga Ha'apai in January 2022. We perform idealised TOMCAT three-dimensional chemical transport model experiments to investigate the impacts if a Hunga-like eruption had been followed by conditions such as the very cold Arctic winter of 2019/2020, and contrast the impact in the cold Antarctic spring of 2020 with the previous warmer, more disturbed year of 2019. In the Antarctic, efficient dehydration by sedimenting ice PSCs limits the impact of a 1 ppmv increase in H_2O to a maximum additional depletion of 16 Dobson Units (DU) in 2020 and 11 DU in 2019 at the vortex edge in late September. A 1 ppmv H_2O increase in the cold Arctic vortex of 2019/2020 causes a maximum of 16 DU additional depletion at the vortex edge in mid March. The direct chemical impact of water vapour from Hunga-like eruption on polar ozone is therefore modest in any given year, given natural variability. However, regular increased H_2O injection or production from increased CH_4 oxidation could represent an important factor in gradual long-terms trends.

1. Introduction

The polar lower stratosphere is one of the coldest environments in the atmosphere. In the Antarctic winter and spring, temperatures are regularly below 195 K, the typical formation threshold of polar stratospheric clouds (PSCs), composed of water vapour and nitric acid (nitric acid trihydrate (NAT), Solomon 1999). Temperatures usually also fall below 188 K, at which point ice PSCs can form and grow large enough to sediment to lower altitudes (e.g. Tritscher et al., 2021). The formation of PSCs allows heterogeneous reactions to activate chlorine, i.e. convert reservoir species such as HCl and $ClONO_2$ to photochemically active species such as Cl_2 and HOCl (Solomon et al., 1986). These species then photolyse to release Cl atoms which can lead to rapid springtime ozone loss through catalytic cycles involving ClO and BrO. At present large ozone depletion regularly occurs every Antarctic spring due to the widespread occurrence of low temperatures and PSCs. Temperatures in the Arctic wintertime lower stratosphere are warmer and more variable than the Antarctic, but occasional years (e.g. 2019/2020) are cold enough for widespread NAT PSC formation and therefore large springtime ozone loss (Manney et al., 2020; Feng et al., 2021).

The discovery of the Antarctic ozone hole (Farman et al., 1985), and its subsequent explanation by Cl/Br chemistry, helped to precipitate and strengthen the Montreal Protocol. This international agreement aims to control the production of the long-lived source gases which deliver the chlorine and bromine to the stratosphere, causing a trend of decreasing ozone in the Antarctic, and to smaller extent the Arctic and mid-latitudes. Examples of these so-called ozone-depleting substances (ODSs) are chlorofluorocarbons (CFCs) and bromine-containing halons. Following successful implementation of the Montreal Protocol, stratospheric chlorine and then bromine peaked in 1990s (see WMO, 2022). This decrease in stratospheric halogen loading has led to the detection of ozone recovery (i.e. decreased depletion by halogens) in the upper stratosphere (Newchurch et al., 2003) and the Antarctic lower stratosphere (Solomon et al., 2016). Evidence for a clear trend in ozone recovery has not yet been detected in other regions due to the slow decay rate of stratospheric chlorine and bromine and the confounding effects of natural variability (e.g. Chipperfield et al., 2017).

Despite action taken under the Montreal Protocol, and the expected long-term recovery of the ozone layer, we continue to experience years with large (even record) ozone depletion in both polar regions. For example, the calendar year 2020 saw extremely large depletion at both poles (Chapter 4 WMO, 2022). There is likely a range of factors in causing continued low polar ozone, some of which are linked to recent extreme phenomena. The large Australian fires around new year 2019/2020 injected smoke particles high into the stratosphere, causing transient perturbations to chemistry and ozone depletion (e.g. Santee et al., 2022; Solomon et al., 2023). The eruption of the underwater Hunga Tonga-Hunga Ha'apai (hereafter Hunga) volcano in January 2022 injected an enormous quantity (150 Tg) of water vapour into the stratosphere (increasing the existing global stratospheric burden by 10%). Note that Hunga only injected a very small amount (0.5 Tg) of SO_2. The additional water vapour is expected to persist in the stratosphere for many years and will impact the ozone layer directly through gas-phase (increased HOx) and heterogeneous chemistry (increased occurrence of PSCs and

View Article Online
DOI: 10.1039/D4FD00163J

changed aerosol activity) chemistry (Santee et al., 2023). Water vapour is also a radiatively active gas. The excess H_2O caused a strong cooling in the SH mid-latitude stratosphere shortly after the eruption (Schoeberl et al., 2022; Vomel et al., 2022), which in turn strengthened the mid-latitude jet and slowed down the Brewer-Dobson Circulation (BDC) (Coy et al., 2022).

Prior to the eruption of Hunga, there had been concern over the impact of future, long-term hydration of the stratosphere, e.g. due to increased methane oxidation or changing tropopause temperatures, on climate, chemistry and polar ozone. von de Gaathen et al. (2021) argued that Arctic ozone depletion in future cold winters through 2100 may increase despite large reductions in chlorine and bromine due to increases in stratospheric water vapour and increased PSC occurrence. In some ways the current Hunga-hydrated stratosphere is a test case for such future conditions.

This paper discusses the impact of a Hunga-like volcanic eruption on polar ozone loss under meteorological conditions experienced in the past 7 years. We use idealised 'counter factual' simulations to explore how ozone would respond under conditions that are optimal for the extensive occurrence of PSCs, for example Arctic winter 2019/2020. In reality, the Hunga water vapour from the January 2022 eruption began to affect Antarctic ozone in 2023 and Arctic ozone in 2023 and 2024. In the case of the Arctic, both of these years were warm and disturbed so the potential for additional PSC occurrence at the critical time for ozone loss (January-March) was limited. For the Antarctic in 2023 efficient dehydration by sedimenting ice clouds appeared to limit the effect on ozone in the vortex core (Wohltmann et al., 2024; Zhou et al., 2024) and may even be a primary route for the removal of this excess water vapour from the stratosphere. Dehydration does not occur to any large extent in the warmer Arctic stratosphere, so this may potentially allow a larger effect from enhanced water vapour.

The layout of the paper is as follows. Section 2 describes the TOMCAT off-line 3-D chemical transport model (CTM) and set-up of the model simulations. Section 3 presents our results for long-term ozone changes and the potential impact of a Hunga-like eruption on different Arctic and Antarctic winters. Section 4 summarises our conclusions.

2. Model Simulations

We have performed a series of experiments with the TOMCAT/SLIMCAT (hereafter TOMCAT) off-line 3-D CTM (Chipperfield, 2006). The model contains a detailed description of stratospheric chemistry, including heterogeneous reactions on sulfate aerosols and PSCs. The model was forced using European Centre for Medium-Range Weather Forecasts (ECMWF) ERA5 winds and temperatures (Hersbach et al., 2020) and run with a resolution of 2.8° × 2.8° with 32 levels from the surface to ~60 km following Dhomse et al. (2019). The surface mixing ratios of long-lived source gases (e.g., CFCs, hydrofluorocarbons, CH_4, N_2O) were taken from WMO (2022) scenario A1. The solar cycle was included using time-varying solar spectral irradiance (SSI) data (1995–2023) from the Naval Research Laboratory (NRL) solar variability model, referred to as NRLSSI2 (update of Coddington et

View Article Online
DOI: 10.1039/D4FD00163J

al., 2016, 2019). Solar fluxes from December 2023 are used to extend the simulation until August 2024. Stratospheric sulfate aerosol surface density (SAD) data until June 2017 were obtained from CMIP6 database ftp://iacftp.ethz.ch/pub_read/luo/CMIP6/ (Arfeuille et al., 2013). From July 2017, we use SAGE-III-based SAD values from Knepp et al. (2024). The implementation of SAD and SSI variability is described in Dhomse et al. (2015) and Dhomse et al. (2016), respectively. The model also has a passive ozone tracer for diagnosing polar chemical ozone loss which is initialised from the chemical ozone tracer every December 1 and June 1 (e.g., Feng et al., 2007).

We performed a total of four model simulations. The control run (**CNTL**) was spun up from 1977 and integrated until August 2024 including all of the processes described above. Sensitivity run **HT** was initialized from CNTL in January 2022 and integrated until June 2024 with a simulation of injection of 150 Tg of H_2O into the stratosphere to mimic Hunga (see Zhou et al., 2024). Run **HT2017** was similar to HT but the Hunga eruption was assumed to occur 5 years earlier in January 2017. This allows us to investigate the impact on a Hunga-like eruption on ozone loss in the cold Arctic winter of 2019/2020. Finally, sensitivity run **EXH2O** was initialised on November 1st 2019 from CNTL but has the instantaneous injection on that date of an additional 1 ppmv water vapour globally, again ahead of the cold Arctic winter of 2019/2020. Run EXH2O allows us to investigate the impact of a uniform additional amount of water vapour in a series of polar winters in a way that is independent of model transport timescales to disperse a localised eruption plume.

We also diagnose the direct chemical impact of the increased H_2O on stratospheric ozone through gas-phase and heterogeneous chemistry. The impacts are simulated with specified realistic meteorology, which is important for temperature-dependent processes such as PSC formation but hence do not account explicitly for dynamical feedbacks. Note that the injection of SO_2 from Hunga is treated as part of the monthly total SAD fields that are read into the model. This is the same for all runs and so in this study we do not diagnose explicitly the impact of this additional SO_2 injection.

3. Results

3.1 Variability of Polar Column Ozone

Ozone levels in the polar winter/spring are maintained by a balance of dynamical and chemical processes. In the Antarctic chemical depletion generally dominates while in the Arctic both processes make large and variable contributions to the column amount in any year. **Figure 1a** shows the mean September Antarctic (60°S-90°S) column ozone from 2004 to 2023 from the Ozone Monitoring Instrument/Ozone Mapping and Profiler Suite (OMI/OMPS) observations and the model runs. From 2004 to 2018 the observed mean column ranges from around 200 DU to 250 DU with some interannual variability and indications of an increasing trend. As discussed by Solomon et al. (2016) this September increase is consistent with a decreasing rate of chlorine- and bromine-catalysed chemical ozone depletion, i.e. ozone recovery due to the actions of the Montreal Protocol. The year

View Article Online
DOI: 10.1039/D4FD00163J

2019 is notable for a large mean September column due to a disturbed polar vortex and increase dynamical replenishment of ozone (see below). Since then, we have experienced a series of four winters (2020-2023) with comparatively low mean column ozone and little interannual variability. This appears to challenge the notion that Antarctic ozone is recovering, but these years do encompass a range of exceptional atmospheric perturbations which likely contributed to lower ozone through either increased chemical depletion or modified transport. Some studies suggest non-negligible chemical depletion of polar ozone caused by the Australian New Year smoke aerosol, with the contribution to ozone loss comparable to that of the sulfate aerosol from the Calbuco eruption in 2015 (Yu et al., 2021; Rieger et al., 2021). The eruption of Hunga in January 2022 is not believed to have impacted Antarctic ozone in 2022 (see discussion of H_2O transport in Section 3.2). For 2023, Zhou et al. (2024) estimated a modest increase in chemical ozone depletion of around 10 DU at the vortex edge due to the increased Hunga water vapour. Interestingly, the impact of the water vapour was limited by dehydration in the vortex core. Regardless of the initial amount of water vapour in the model vortex, formation and sedimentation of ice PSCs removes all of the gas-phase H_2O except for a residual amount determined by the equilibrium vapour pressure.

Figure 2a shows mean March Arctic (60°N-90°N) column ozone from observations and our model simulations from 2004 to 2024. The OMI/OMPS observations clearly show 2020 (330 DU) and 2011 (335 DU) as the 2 years with extremely low column ozone with, by this metric, slightly lower values in 2020. The low ozone in these cold years was caused by increased PSC activity and related chemical ozone loss, coupled with smaller dynamical replenishment (see e.g. Wohltmann et al., 2020; Feng et al., 2021). In recent years the mean Arctic column was relatively small in 2021 and 2022, larger in 2023 and then exceptionally large in 2024 (Newman et al., 2024).

The chemical ozone tracer from model run CNTL captures the overall interannual variability in both polar regions very well (**Figures 1a** and **2a**). Results from the model run can be used to separate the contributions of dynamics and transport, for example by comparing the passive ozone tracer between the start of winter (July in Antarctic, December in Arctic) with late spring. These differences show that much of the interannual variability in springtime column ozone, averaged over these wide latitude bands, is determined by transport (e.g. 2019 in the Antarctic, 2010/2011 and 2019/2020 in the Arctic).

3.2 Transport of Hunga water vapour

Figure 3 shows the zonal mean monthly mean H_2O anomalies after the Hunga injection in model run **HT** compared with Microwave Limb Sounder (MLS) measurements (Millan et al., 2024) for selected months until April 2024 (updated from Zhou et al., 2021). The model successfully captures many aspects of the transport of the Hunga H_2O over this time period. While the injected total mass in the model is consistent with MLS, the simulation has slightly larger peak anomalies and smaller horizontal extent after injection. The simulated plume

View Article Online
DOI: 10.1039/D4FD00163J

spread is in very good agreement with the SH observations through 2024, in particular regarding the characteristics and behaviour of the excess H_2O at the mixing barriers in the stratosphere, including the Antarctic vortex edge and the subtropics. Around 4-6 months after the eruption, the excess H_2O moves into the Southern Hemisphere (SH) mid-latitudes within the shallow branch of the BDC. However, it does not intrude into the 2022 Antarctic polar vortex due to the strong polar night jet at the vortex edge. Only after the breakdown of the Antarctic polar vortex in November 2022 did the H_2O reach the pole (Manney et al., 2023). The subtropical transport barrier in 2022 summer, favoured by weak wave forcing in the easterly phase of the Quasi-Biennial Oscillation, confines the excess H_2O to the SH, until the transition to westerlies at the end of 2022. This also explains the improvement of the model in 2023 compared with 2022 in representing the H_2O transport across the equator. H_2O enters the deep branch of the BDC in 2023, ascending from the tropics and descending into the high latitudes in the SH. The model reproduces well the timing of the Hunga-injected H_2O penetrating the polar vortex, and the altitudes of the H_2O plume. This indicates that the model has a good representation of both the poleward horizontal H_2O transport by the shallow branch of the BDC and the ascent of the water-enriched air to high levels by the deep branch of the BDC.

In contrast, the arrival of the Hunga H_2O in the Northern Hemisphere (NH) is not simulated as well as the SH. Comparison of the highlighted 1 ppmv contour (**Figure 3**) shows that this level of water vapour reaches the Arctic lower stratosphere in mid-2023 in the MLS data; in the model the additional H_2O in this region is still less than this value in spring 2024. To overcome this issue we also performed simulation EXH2O which imposes a uniform 1 ppmv increase in H_2O.

3.3 Impact of Increased Water Vapour on Polar Ozone

As discussed in Section 1, increased stratospheric water vapour is expected to lead to additional polar ozone loss through increased occurrence of PSCs. **Figure 4** quantifies this chemical effect for the model run with the realistic timing of the Hunga eruption (HT) and the run with the eruption assumed to occur in January 2017 (HT2017). For both runs the column ozone depletion starts in the southern mid-latitudes and reaches the Antarctic polar vortex around 18 months after eruption (i.e. 2023 for run HT) and the Arctic around two years after eruption. The modelled mean impact in the Antarctic maximises at around 10 DU at the vortex edge (65°S) and decreases as H_2O is removed from the model stratosphere with an e-folding time of around 4 years (Zhou et al., 2024) (**Figure 1b**). In the Arctic the largest impact occurs in run HT2017 in early 2020, i.e. as expected in the very cold Arctic vortex of that year (see **Figure 2b**).

3.3.1 Antarctic winter/springs of 2019 and 2020

View Article Online
DOI: 10.1039/D4FD00163J

The impact of the increased water vapour in model runs HT2017 and EXH2O on NAT and ice PSC occurrence in Antarctic winters 2019 and 2020 is shown in **Figures 5a** and **b**. Clearly, as NAT forms at a higher temperature than ice (195 K versus 188 K), it has an earlier onset and more extensive coverage. The additional PSC occurrence compared to control run CNTL is small but most pronounced in early winter. As noted by Zhou et al. (2024), efficient dehydration the model vortex core after the onset of ice PSCs in June removes most of the additional water vapour. This is confirmed by the modelled time series of water vapour for the two years (**Figures 6e** and **7e**). The excess mean water vapour in May is removed so that by September the model runs CNTL, HT2017 and EXH2O all have similar mean mixing ratios. This difference in early PSC occurrence has only a small effect of chlorine processing (**Figures 6a-d** and **7a-d**). Again, the largest differences in the areal mean occur in early winter. By late winter and spring, the main period for ozone loss, the extent of activation is similar in the three simulations.

Figures 8 and **9** show the impact on column ozone of the additional H_2O on two example days in late September 2019 and 2020. The largest additional depletion occurs at the edge of the polar vortex where the PSC occurrence is not saturated, and dehydration is not extensive. In the warmer, more disturbed vortex of 2019 the approximately 1 ppmv additional H_2O (**Figure 6e**) in run HT2017 causes a maximum additional O_3 depletion of 11 DU (**Figure 8d**). In 2020 the additional H_2O in run HT2017 is reduced to 0.4 ppmv (**Figure 7e**) and the column impact is only 8 DU. In contrast, the additional 1 ppmv H_2O in run EXH2O causes a depletion of an additional 16 DU (**Figure 9e**). For polar-cap-mean ozone these impacts translate to September-mean depletion in run HT2017 of 11 DU in 2018 (not discussed above), 7 DU in 2019 and 3 DU in 2020. Run EXH2O produces additional depletion of 8 DU in 2020 (**Figure 1b**).

3.3.2 Arctic Ozone

Figure 2a summarised the observed mean March column ozone in recent years and indicates how Arctic ozone levels depend on the occurrence of low temperatures. Both the 2022/2023 and 2023/2024 Arctic ozone loss seasons showed comparatively warm conditions in the polar vortex in spring relative to the long-term climatology. These conditions are unfavourable for ozone loss initiated by heterogeneous reactions, preventing a significant effect from the Hunga eruption on ozone depletion in these years. While the 2022/2023 Arctic winter started with temperatures below the long-term average in January 2023, a major sudden stratospheric warming (SSW) on February 16th, 2023 caused the vortex to break up by the end of February, before chlorine-catalysed ozone loss could have a major effect (Druckenmiller et al., 2024). Although the 2023/2024 Arctic winter was initially unusually cold, it was characterised by an early major SSW on 16 January, from which the vortex recovered, and a second major SSW on March 4th that caused an early breakup of the vortex (see Newman et al., 2024).

Given the nature of the Arctic winters since the Hunga eruption here we look at the potential for a larger impact during a cold Arctic winter. We therefore use TOMCAT to simulate the

View Article Online
DOI: 10.1039/D4FD00163J

impact that Hunga could have had on the cold Arctic winter of 2019/2020 through simulation HT2017. In order to allow the modelled H_2O injection to reach the Arctic (given the slower than observed interhemispheric transport shown in **Figure 3**) we inject the H_2O in 2017, 3 years ahead of the target winter. To circumvent uncertainty in the timing of H_2O transport, in run EXH2O we simply increase model H_2O globally by 1 ppmv in November 2019.

In contrast to the Antarctic, the occurrence of ice PSCs in the Arctic is rare. The additional water vapour in runs HT2017 and EXH2O at the start of winter is maintained through to spring (**Figure 10e**). There appear to be two small signals of dehydration around early December in all 3 runs and in late January, especially in run EXH2O. This January event is reflected in the larger scale occurrence of ice PSCs across the polar region (**Figure 5c**) This lack of dehydration could potentially allow the additional H_2O to have a larger impact in a cold Arctic winter than in the dehydrated Antarctic. However, the impact of NAT occurrence in run EXH2O compared to run CNTL is small. The corresponding impact on chlorine activation and polar cap ozone is also small.

The largest column ozone depletion modelled on March 21st 2020 is 3 DU at the vortex edge in run HT2017 and 16 DU in run EXH2O with the large H_2O perturbation (**Figure 11**). The polar cap March mean ozone impacts for 2020 are around 2 DU and 9 DU, respectively (**Figure 2b**), with a decreasing impact in later warmer years with less additional H_2O.

4. Conclusions

We have performed a series of three-dimensional model experiments to investigate the impacts of a large injection of water vapour into the stratosphere on polar ozone depletion. These simulations mimic some details of a Hunga-like underwater volcanic eruption. In particular, we investigated the potential impact of increased water vapour in cold Antarctic and Arctic winters, through increased PSC occurrence.

As noted by previous studies (e.g. Wohltmann et al., 2023; Zhou et al., 2024) efficient Antarctic dehydration by sedimenting ice PSCs limits the impact of an example additional 1 ppmv H_2O to a maximum additional depletion of 16 DU in 2020 and 11 DU in 2019 at the vortex edge in late September. Similar dehydration does not occur in the warmer Arctic, even in the extreme cold conditions of 2019/2020. Under these conditions an additional 1 ppmv H_2O causes a maximum of 16 DU additional depletion at the vortex edge in mid March. Note that our simulations only diagnose the direct chemical impact of the increased water vapour. As an important climate gas, changes in stratospheric water vapour will lead to changes in temperature and circulation which can also have an impact on column ozone in different regions.

Our model results shows that direct chemical impact of water vapour from a large Hunga-like eruption (which would produce increases of less than 1 ppmv after large-scale spreading of the plume) would be small compared to observed interannual variability in springtime column ozone (Fleming et al., 2024), especially in the Arctic. However, should increases in

stratospheric water vapour be sustained this additional depletion could be important for long-term trends. Such hydration could occur, for example, through warmer tropical tropopause temperatures or through increasing levels of stratospheric methane, which produces H_2O on oxidation.

Finally, is worth noting, that around 40 years after the discovery of the ozone hole, and after over 20 years since stratospheric chlorine and bromine started to decline, we are still experiencing very large ozone depletion at both poles. These low levels are related, at least in part, to a series of exceptional events such as wildfire smoke and volcanic eruptions. Nevertheless, these events and state of the ozone layer emphasise the need for continued observations, laboratory studies and chemistry-climate modelling of the stratosphere (see Chipperfield and Bekki, 2024).

Conflict of Interest: The authors declare no conflicts of interest.

Acknowledgements: MPC and SSD were supported by the NCEO TerraFIRMA, NERC LSO3 (NE/V011863/1) and ESA OREGANO (4000137112/22/I-AG) projects. WF was supported by the NCAS Long-Term Science programme (NE/ R015244/1). XZ was supported by the National Natural Science Foundation of China (42275059, 12411530093).

Author Contributions: Conceptualization: MPC. Methodology: MPC. Formal analysis: SF, SSD, WF, XZ, MPC. Writing – original draft: MPC. Writing – review and editing: all coauthors.

Data availability: The OMI/OMPS data is available from https://ozonewatch.gsfc.nasa.gov/meteorology/figures/ozone
The MLS data is available from https://mls.jpl.nasa.gov/

References

Arfeuille, F., Luo, B. P., Heckendorn, P., Weisenstein, D., Sheng, J. X., Rozanov, E., et al., Modeling the stratospheric warming following the Mt. Pinatubo eruption: uncertainties in aerosol extinctions. *Atmos. Chem. Phys.*, **13**, 11221–11234. https://doi.org/10.5194/acp-13-11221-2013, 2013.

Chipperfield, M., New version of the TOMCAT/SLIMCAT off-line chemical transport model: Intercomparison of stratospheric tracer experiments. *The Quarterly Journal of the Royal Meteorological Society*, **132**, 1179–1203. https://doi.org/10.1256/qj.05.51, 2006.

Chipperfield, M. P., Bekki, S., Dhomse, S., Harris, N. R. P., Hassler, B., Hossaini, R., et al., Detecting recovery of the stratospheric ozone layer. *Nature*, **549**, 211–218. https://doi.org/10.1038/nature23681, 2017.

Chipperfield, M.P., and S. Bekki, Opinion: Stratospheric ozone – Depletion, recovery and new challenges, *Atmos. Chem. Phys.*, **24**, 2783-2802, doi:10.5194/acp-24-2783-2024, 2024.

Coddington, O., Lean, J., Pilewskie, P., Snow, M., & Lindholm, D., A solar irradiance climate data record. *Bulletin of the American Meteorological Society*, **97**, 1265–1282. https://doi.org/10.1175/BAMS-D-14-00265.1, 2016.

Coddington, O., Lean, J., Pilewskie, P., Snow, M., Richard, E., Kopp, G., et al. Solar Irradiance variability: comparisons of models and measurements. *Earth and Space Science*, **6**, 2525–2555. https://doi.org/10.1029/2019EA000693, 2019.

Coy, L., Newman, P. A., Wargan, K., Partyka, G., Strahan, S. E., & Pawson, S., Stratospheric circulation changes associated with the Hunga Tonga - Hunga Ha'apai eruption. *Geophys. Res. Lett.*, **49**, e2022GL100982. https://doi.org/10.1029/2022GL100982, 2022.

Dhomse, S., Chipperfield, M. P., Damadeo, R. P., Zawodny, J. M., Ball, W. T., Feng, W., et al., On the ambiguous nature of the 11-year solar cycle signal in upper stratospheric ozone. *Geophys. Res. Lett.*, **43**, 7241–7249. https://doi.org/10.1002/2015GL069958, 2016.

Dhomse, S., Chipperfield, M. P., Feng, W., Hossaini, R., Mann, G. W., & Santee, M. L., Revisiting the hemispheric asymmetry in mid-latitude ozone changes following the Mount Pinatubo eruption: A 3-D model study. *Geophys. Res. Lett.*, **42,** 3038–3047. https://doi.org/10.1002/2015GL063052, 2015.

Dhomse, S. S., Feng, W., Montzka, S. A., Hossaini, R., Keeble, J., McQuaid, J., et al., Delay in recovery of the Antarctic ozone hole from unexpected CFC-11 emissions. *Nature Communications*, **10**, 5781. https://doi.org/10.1038/s41467-019-13717-x, 2019.

Druckenmiller, M.L., R.L. Thoman, and T.A. Moon, Eds., The Arctic [in "State of the Climate in 2023"]. *Bulletin of the American Meteorological Society*, **105**, S277–S330, doi: 10.1175/BAMS-D-24-0101.1, 2024.

Farman, J. C., Gardiner, B. G. & Shanklin, J. D.: Large losses of total ozone in Antarctica reveal seasonal ClOx/NOx interaction, *Nature*, **315**, 207–210, doi:10.1038/315207a0, 1985.

Feng, W., Chipperfield, M. P., Davies, S., von der Gathen, P., Kyrö, E., Volk, C. M., et al. Large chemical ozone loss in 2004/2005 Arctic winter/spring. *Geophys. Res. Lett.*, **34**, L09803. https://doi.org/10.1029/2006GL029098, 2007.

Feng, W., S.S. Dhomse, C. Arosio, M. Weber, J.P. Burrows, M.L. Santee and M.P. Chipperfield, Arctic ozone depletion in 2019/20: Roles of chemistry, dynamics and the Montreal Protocol, *Geophys. Res. Lett.*, **48**, e2020GL091911, doi:10.1029/2020GL091911, 2021.

Fleming, E.L., P.A. Newman, Q. Liang, and L.D. Oman, Stratospheric temperature and ozone impacts of the Hunga Tonga-Hunga Ha'apai water vapor injection. *J. Geophys. Res.*, **129**, e2023JD039298, doi: 10.1029/2023JD039298, 2024.

Hersbach, H., Bell, B., Berrisford, P., Hirahara, S., H, A., M, J., et al., The ERA5 global reanalysis. *The Quarterly Journal of the Royal Meteorological Society*, **146**, 1999–2049. https://doi.org/10.1002/qj.3803, 2020.

Knepp, T. N., Kovilakam, M., Thomason, L., and Miller, S. J.: Characterization of stratospheric particle size distribution uncertainties using SAGE II and SAGE III/ISS extinction spectra, *Atmos. Meas. Tech.*, **17**, 2025–2054, https://doi.org/10.5194/amt-17-2025-2024, 2024.

Manney, G. L., Livesey, N. J., Santee, M. L., Froidevaux, L., Lambert, A., Lawrence, Z. D., et al., Record-low Arctic stratospheric ozone in 2020: MLS observations of chemical processes and comparisons with previous extreme winters. *Geophys. Res. Lett.*, **47**, e2020GL089063. https://doi.org/10.1029/2020GL089063, 2020.

Manney, G.L., M.L. Santee, A. Lambert, L.F. Millán, K. Minschwaner, F. Werner, Z.D. Lawrence, W.G. Read, N.J. Livesey, and T. Wang, Siege in the southern stratosphere: Hunga Tonga-Hunga Ha'apai water vapor excluded from the 2022 Antarctic polar vortex. *Geophys. Res. Lett.*, **50**, e2023GL103855, doi: 10.1029/2023GL103855, 2023.

Millán, L., W.G. Read, M.L. Santee, A. Lambert, G.L. Manney, J.L. Neu, M.C. Pitts, F. Werner, N.J. Livesey, and M.J. Schwartz, The evolution of the Hunga hydration in a moistening stratosphere. *Geophys. Res. Lett.*, **51**, e2024GL110841, doi: 10.1029/2024GL110841, 2024.

Newchurch, M. J., Yang, E.-S., Cunnold, D. M., Reinsel, G. C., Zawodny, J. M., & Russell, J. M., Evidence for slowdown in stratospheric ozone loss: First stage of ozone recovery. *J. Geophys. Res.*, **108**, 4507. https://doi.org/10.1029/2003JD003471, 2003.

Newman, P. A., Lait, L. R., Kramarova, N.A., Coy, L., Frith, S. M., Oman, L. D., & Dhomse, S. S. Record high march 2024 Arctic total column ozone. *Geophys. Res. Lett.*, **51**, e2024GL110924. https://doi.org/10.1029/2024GL11092, 2024.

Rieger, L.A., W.J. Randel, A.E. Bourassa, and S. Solomon, Stratospheric temperature and ozone anomalies associated with the 2020 Australian New Year fires, *Geophys. Res. Lett.*, **48**, e2021GL095898, doi:10.1029/2021GL095898, 2021.

Santee, M. L., Lambert, A., Manney, G. L., Livesey, N. J., Froidevaux, L., Neu, J. L., et al.: Prolonged and pervasive perturbations in the composition of the Southern Hemisphere midlatitude lower stratosphere from the Australian New Year's fires, *Geophys. Res. Lett.*, 49, e2021GL096270. https://doi.org/10.1029/2021GL096270, 2022.

Santee, M.L., A. Lambert, L. Froidevaux, G.L. Manney, M.J. Schwartz, L.F. Millán, N.J. Livesey, W.G. Read, F. Werner, and R.A. Fuller, Strong evidence of heterogeneous processing on stratospheric sulfate aerosol in the extrapolar Southern Hemisphere following the 2022 Hunga Tonga-Hunga Ha'apai eruption. *J. Geophys. Res.*, **128**, e2023JD039169, doi: 10.1029/2023JD039169, 2023.

Schoeberl, M. R., Wang, Y., Ueyama, R., Taha, G., Jensen, E., & Yu, W., Analysis and impact of the Hunga Tonga - Hunga Ha'apai stratospheric water vapor plume. *Geophys. Res. Lett.*, **49**, e2022GL100248. https://doi.org/10.1029/2022GL100248, 2022.

Solomon, S.: Stratospheric ozone depletion: a review of concepts and history, *Rev. Geophys.*, **37**, 275–316, doi:10.1029/1999RG900008, 1999.

Solomon, S., Garcia, R. R., Rowland, F. S. & Wuebbles, D. J.: On the depletion of Antarctic ozone, *Nature*, **321**, 755–758, doi:10.1038/321755a0, 1986.

Solomon, S., Ivy, D. J., Kinnison, D., Mills, M. J., Neely, R. R., & Schmidt, A., Emergence of healing in the Antarctic ozone layer. *Science*, **353**, 269–274. https://doi.org/10.1126/science.aae0061, 2016.

Solomon, S., Stone, K., Yu, P., Murphy, D.M., Kinnison, D., Ravishankara, A.R., and Wang, P.: Chlorine activation and enhanced ozone depletion induced by wildfire aerosol, *Nature*, **615**, 10.1038/s41586-022-05683-0, 2023.

Tritscher, I., M.C. Pitts, L.R. Poole, S.P. Alexander, F. Cairo, M.P. Chipperfield, J.-U. Grooss, M. Hoepfner, A. Lambert, B.P. Luo, S. Molleker, A. Orr, R. Salawitch, M. Snels, R. Spang, W. Woiwode and T. Peter, Polar stratospheric clouds: Satellite observations, processes, and role in ozone depletion, *Rev. Geophys.*, **59**, e2020RG000702, doi:10.1029/2020RG000702, 2021.

Vomel, H., Evan, S., & Tully, M., Water vapor injection into the stratosphere by Hunga Tonga - Hunga Ha'apai. *Science*, *377*(6613), 1444-1447. https://doi.org/10.1126/science.abq2299, 2022.

von der Gathen, P., R. Kivi, I. Wohltmann, R.J. Salawitch, and M. Rex, Climate change favours large seasonal loss of Arctic ozone, *Nat. Commun.,* **12,** 3886, doi:10.1038/s41467-021-24089-6, 2021.

WMO Scientific assessment of ozone depletion: 2022. Global Ozone Research and Monitoring Project – GAW Report no. 278. Geneva, Switzerland: World Meteorological Organization, 2022.

Wohltmann, I., von der Gathen, P., Lehmann, R., Maturilli, M., Deckelmann, H., Manney, G. L., et al. Near-complete local reduction of Arctic stratospheric ozone by severe chemical loss in spring 2020. *Geophys. Res. Lett.*, **47**, e2020GL089547. https://doi.org/10.1029/2020GL089547, 2020.

Wohltmann, I., M.L. Santee, G.L. Manney, and L.F. Millán, The chemical effect of increased water vapor from the Hunga Tonga-Hunga Ha'apai eruption on the Antarctic ozone hole. *Geophys. Res. Lett.*, **51**, e2023GL106980, doi: 10.1029/2023GL106980, 2024.

Yu, P., S.M. Davis, O.B. Toon, R.W. Portmann, C.G. Bardeen, J.E. Barnes, H. Telg, C. Maloney, and K.H. Rosenlof, Persistent stratospheric warming due to 2019– 2020 Australian wildfire smoke, *Geophys. Res. Lett.*, **48**, e2021GL092609, doi:10.1029/2021GL092609, 2021.

Zhou, X., S.S. Dhomse, W. Feng, G. Mann, S. Heddell, H. Pumphrey, B.J. Kerridge, B. Latter, R. Siddans, L. Ventress, R. Querel, P. Smale, E. Asher, E.G. Hall, S. Bekki and M.P. Chipperfield, Antarctic vortex dehydration in 2023 as a substantial removal pathway for Hunga Tonga-Hunga Ha'apai water vapour, *Geophys. Res. Lett.*, **51**, e2023GL107630, doi:10.1029/2023GL107630, 2024.

Figures

View Article Online
DOI: 10.1039/D4FD00163J

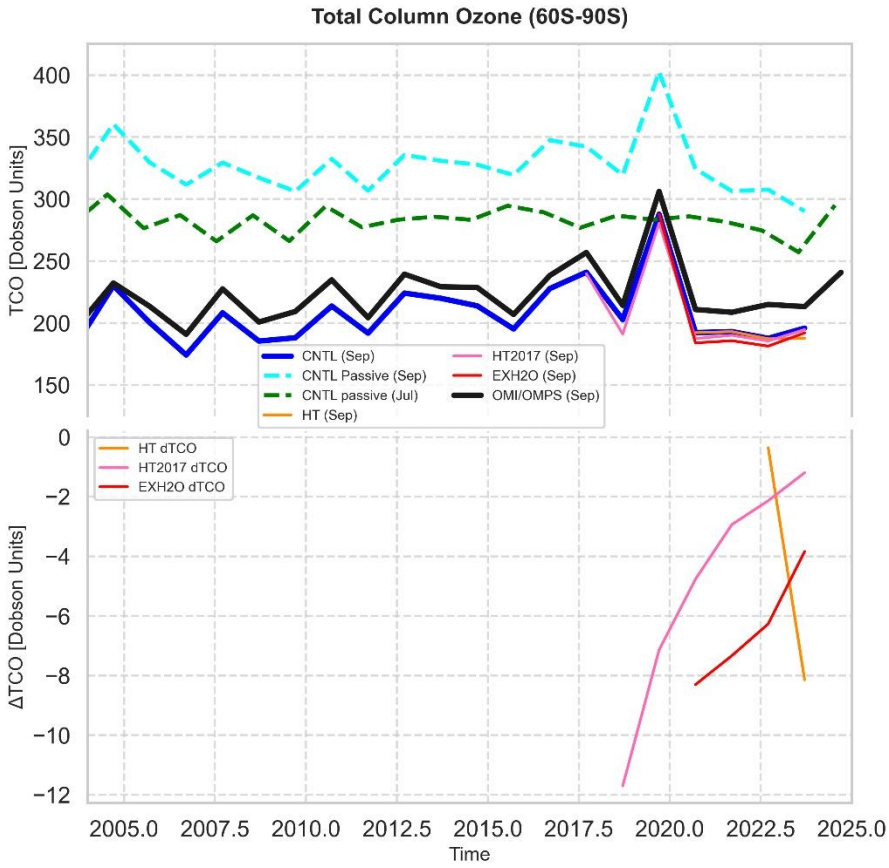

Figure 1. Antarctic (60°–90°S, geographical latitude) monthly mean column ozone (DU) from 2004 to 2023. The upper panel (a) shows September OMI/OMPS observations and model simulations CNTL, HT (2022 on), HT2017 (2017 on) and EXH2O (2019 on). The dashed lines show the passive ozone from CNTL for September (blue) and the previous July (green). The lower panel (b) shows the difference in mean October ozone (DU) between runs CNTL and HT, HT2017 and EXH2O. Updated and adapted from Feng et al. (2021).

View Article Online
DOI: 10.1039/D4FD00163J

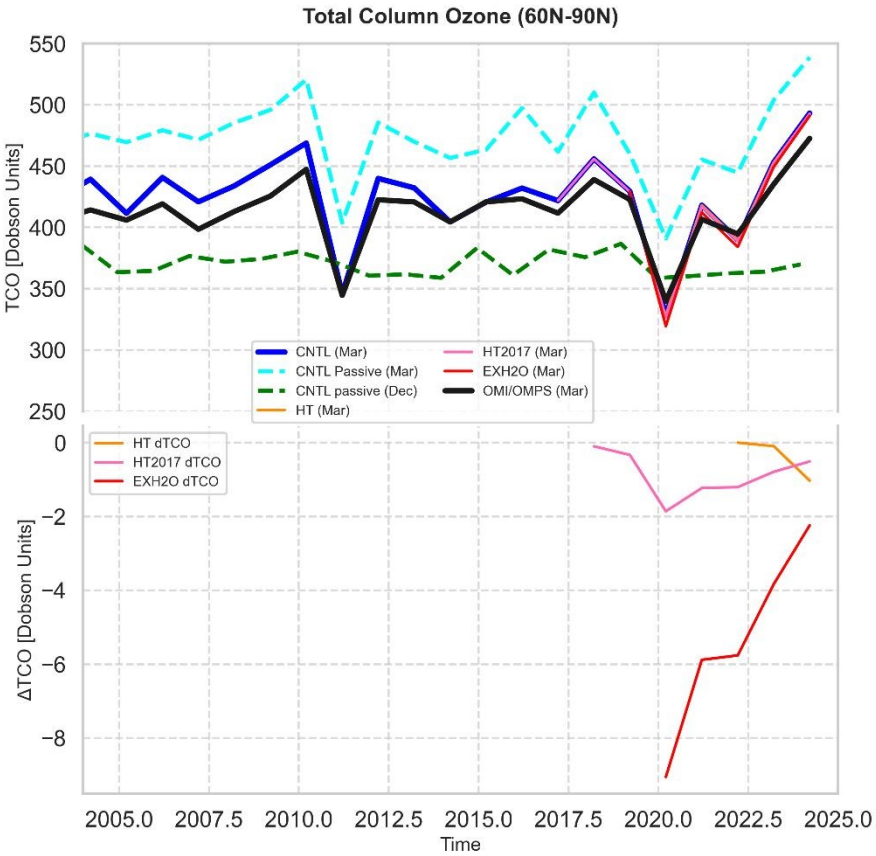

Figure 2. As **Figure 1** but for the Arctic (60°–90°N, geographical latitude) monthly mean March column ozone (DU) from 2004 to 2024. The upper panel (a) shows OMI/OMPS observations and model simulations CNTL, HT, HT2017 and EXH2O. The dashed lines show the passive ozone from CNTL for March (blue) and the previous December (green). The lower panel (b) shows the difference in mean March column ozone (DU) between run CNTL and runs HT, HT2017 and EXH2O. Updated and adapted from Feng et al. (2021).

View Article Online
DOI: 10.1039/D4FD00163J

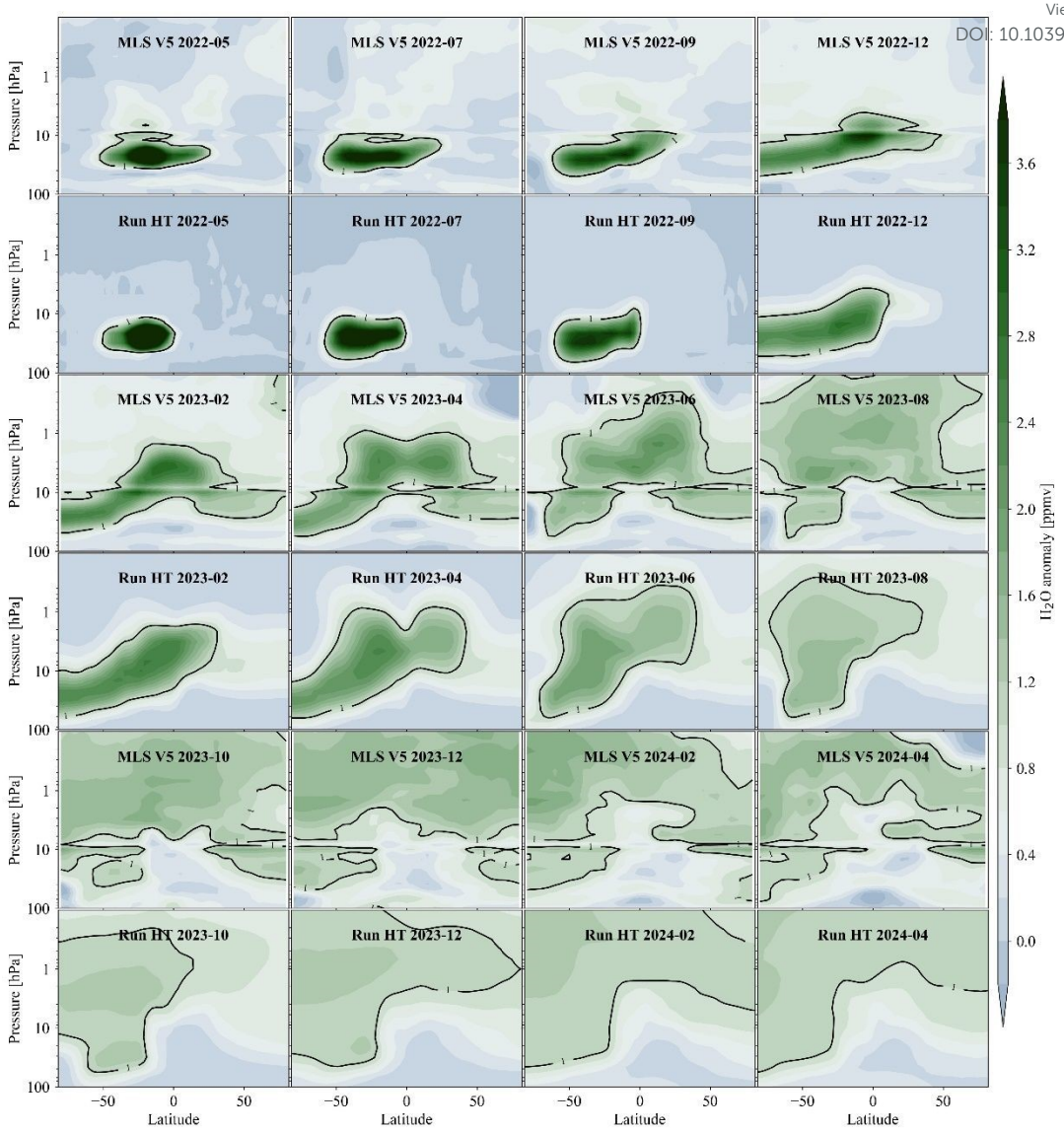

Figure 3. Water vapour (H_2O) evolution after the Hunga eruption. Zonal mean latitude-pressure cross sections of H_2O anomalies observed by MLS v5 and simulated by model run HT from May 2022 to April 2024. Updated from Figure 1b of Zhou et al. (2024).

View Article Online
DOI: 10.1039/D4FD00163J

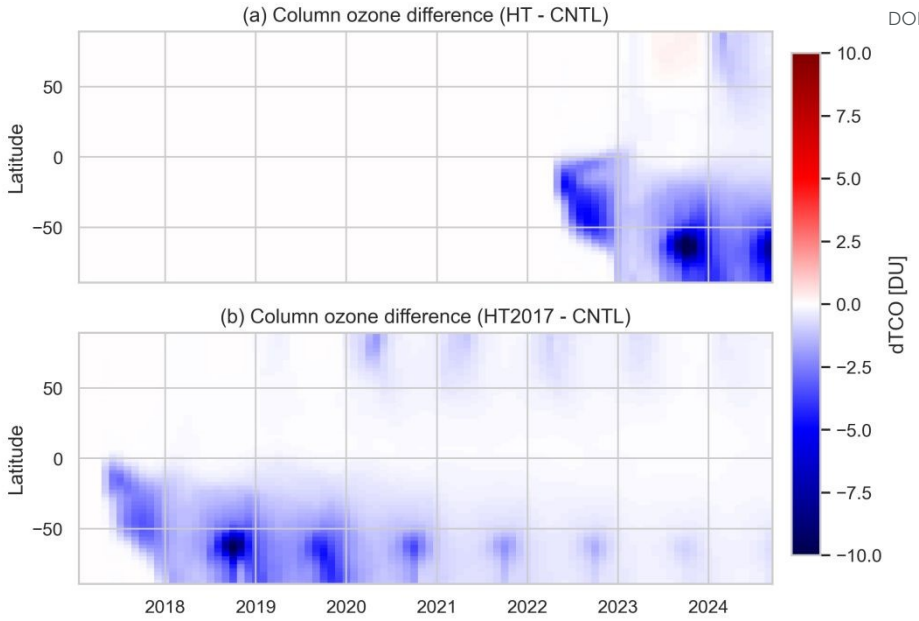

Figure 4. Latitude-time series of column ozone (DU) difference for runs (a) HT and (b) run HT2017 compared to control run CNTL from 2017 to August 2024.

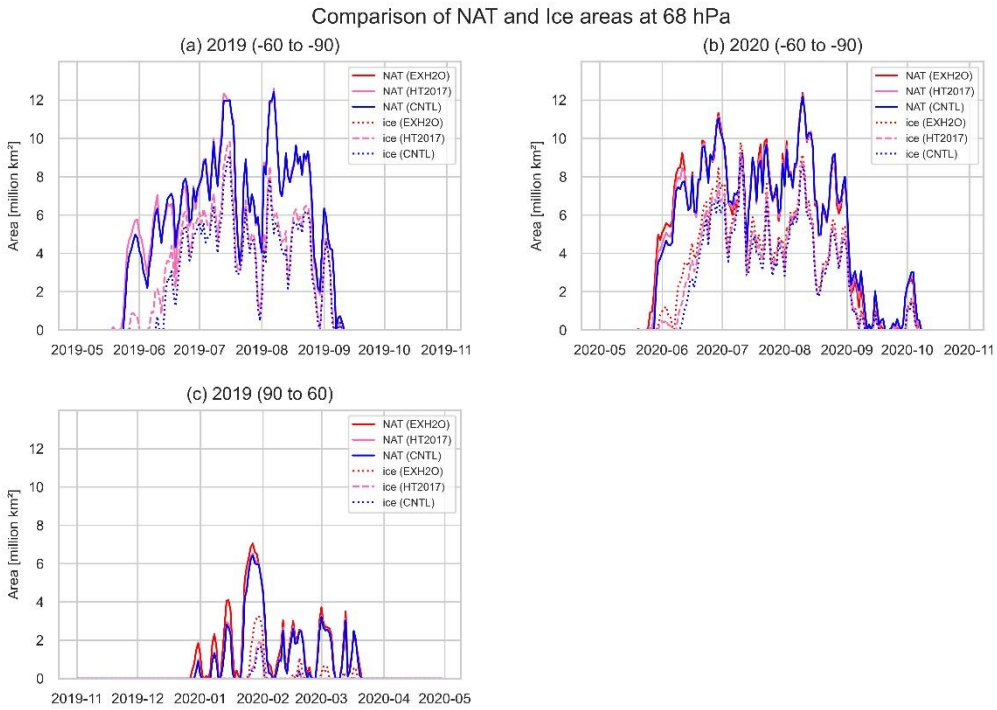

Figure 5. Extent of polar stratospheric cloud (PSC) area (million km^2) for nitric acid trihydate (NAT) and ice particles at 68 hPa from model runs CNTL, HT2017 and EXH2O for (a) 60°S-90°S in 2019, (b) 60°S-90°S in 2020, and (c) 60°N-90°N in 2019/2020.

View Article Online
DOI: 10.1039/D4FD00163J

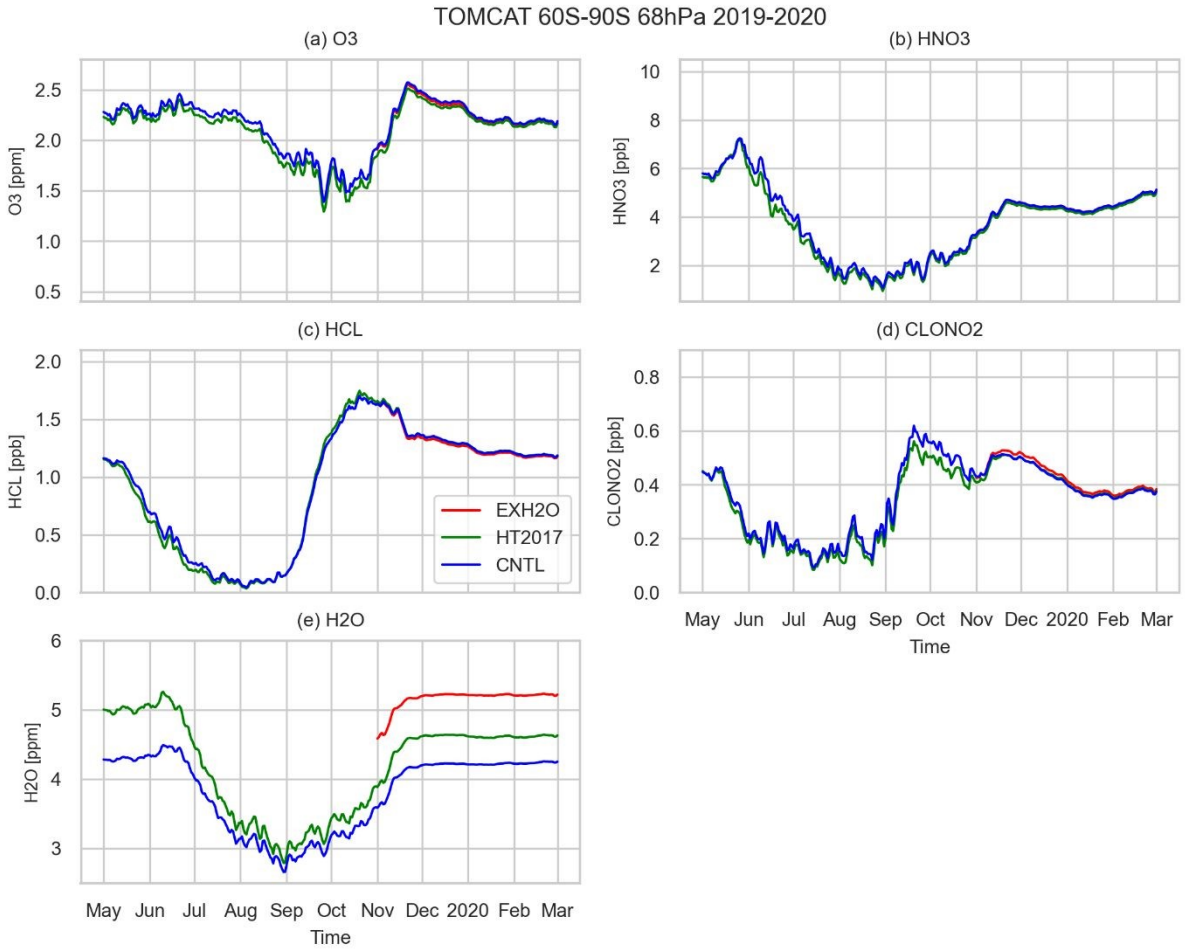

Figure 6. Mean volume mixing ratios for 60°S-90°S for May 2019 to February 2020 at 68 hPa from model runs CNTL, HT2017 and EXH2O (November 2019 onwards) for (a) O_3, (b) HNO_3, (c) HCl, (d) $ClONO_2$ and (e) H_2O.

View Article Online
DOI: 10.1039/D4FD00163J

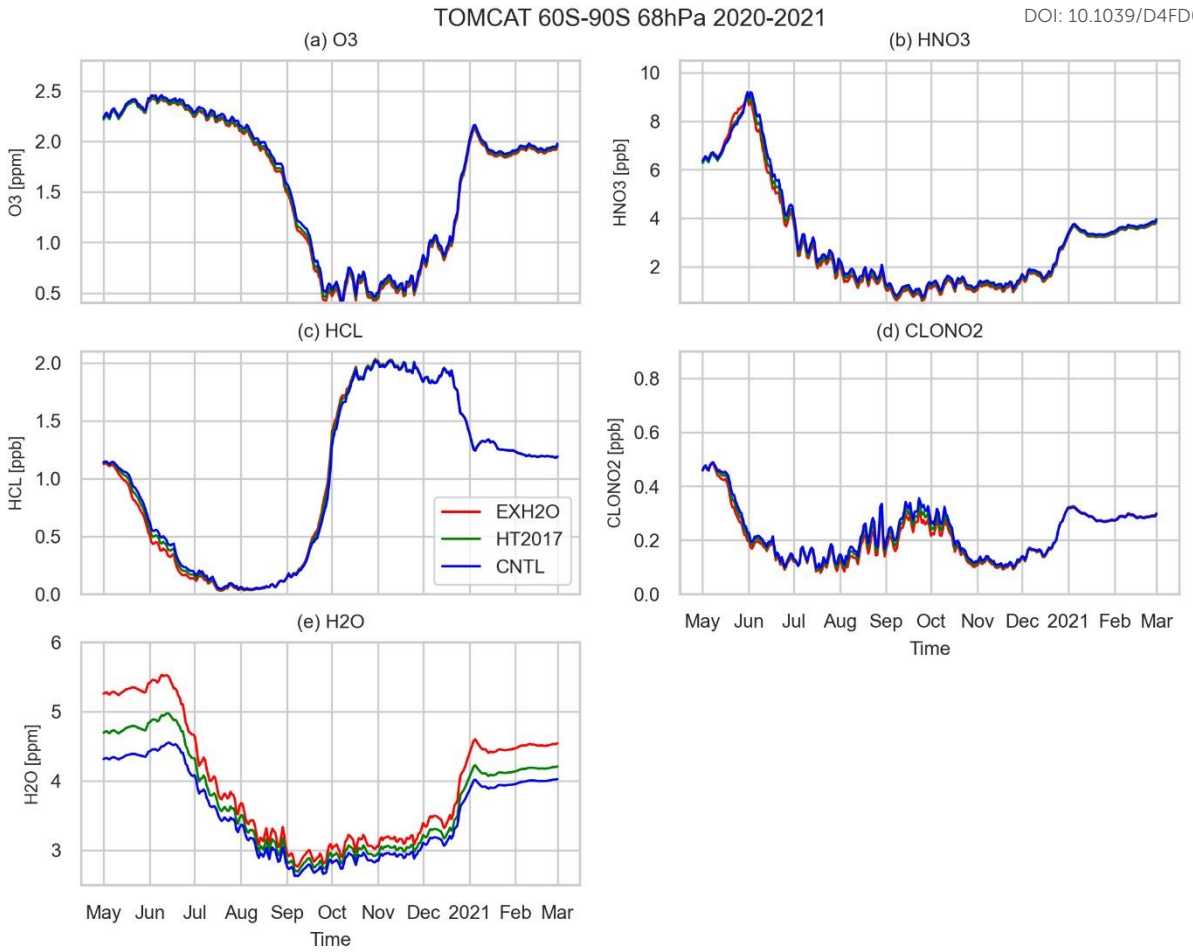

Figure 7. Mean volume mixing ratios for 60ºS-90ºS for May 2020 to February 2021 at 68 hPa from model runs CNTL, HT2017 and EXH2O for (a) O_3, (b) HNO_3, (c) HCl, (d) $ClONO_2$ and (e) H_2O.

View Article Online
DOI: 10.1039/D4FD00163J

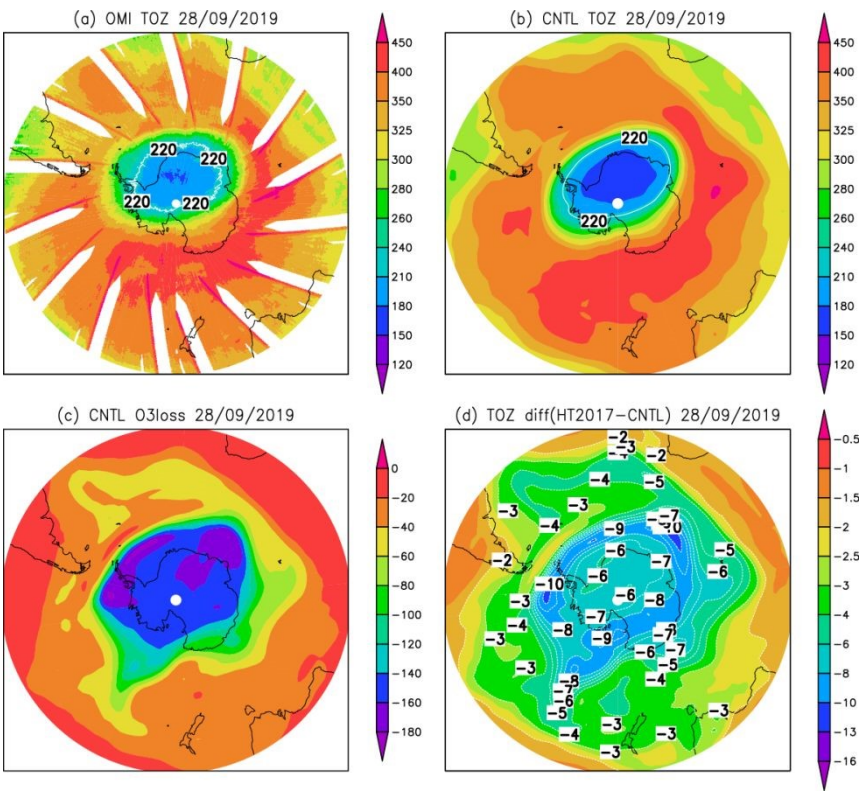

Figure 8. Total column ozone (DU) on September 28, 2019 (a) observed by OMI, (b) from model run CNTL, (c) chemical ozone loss (DU) from run CNTL (active minus passive) and (d) difference in column ozone (DU) between runs HT2017 and CNTL. In panels (a) and (b) the 220 DU contour is indicated in white.

View Article Online
DOI: 10.1039/D4FD00163J

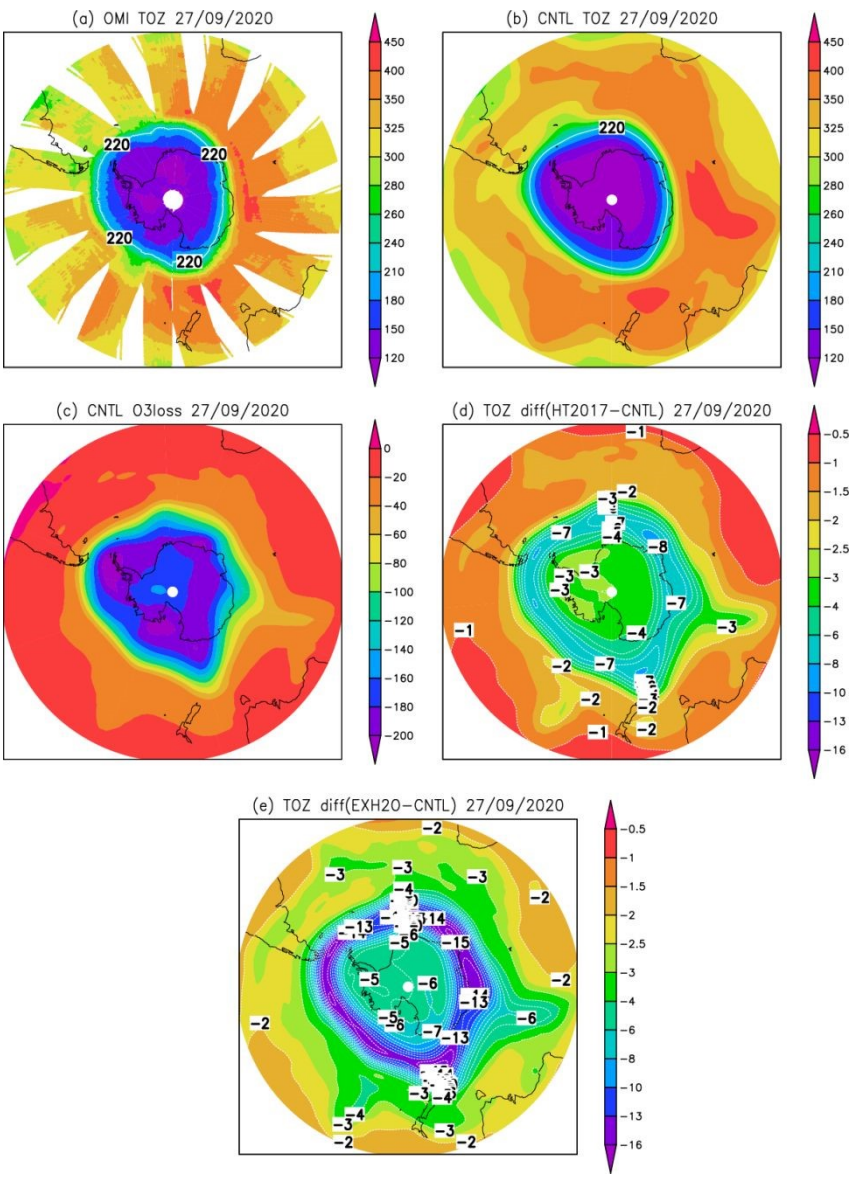

Figure 9. Total column ozone (DU) on September 27, 2020 (a) observed by OMI, (b) from model run CNTL, (c) chemical ozone loss (DU) from run CNTL (active minus passive), (d) difference in column ozone (DU) between runs HT2017 and CNTL and (e) difference in column ozone (DU) between runs EXH2O and CNTL. In panels (a) and (b) the 220 DU contour is indicated in white.

View Article Online
DOI: 10.1039/D4FD00163J

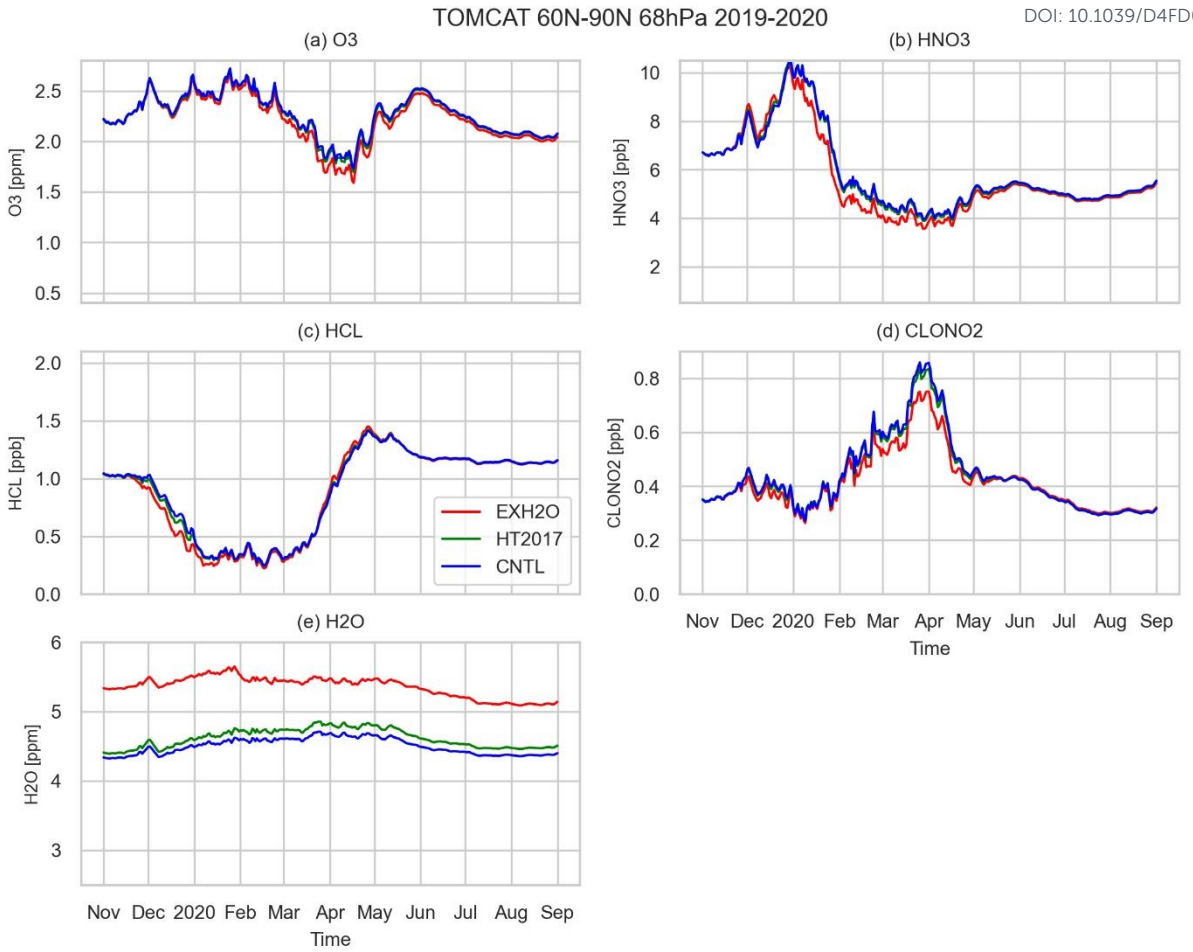

Figure 10. Mean volume mixing ratios (ppmv) for 60°N-90°N for November 2019 to August 2020 at 68 hPa from model runs CNTL, HT2017 and EXH2O for (a) O_3, (b) HNO_3, (c) HCl, (d) $ClONO_2$ and (e) H_2O.

View Article Online
DOI: 10.1039/D4FD00163J

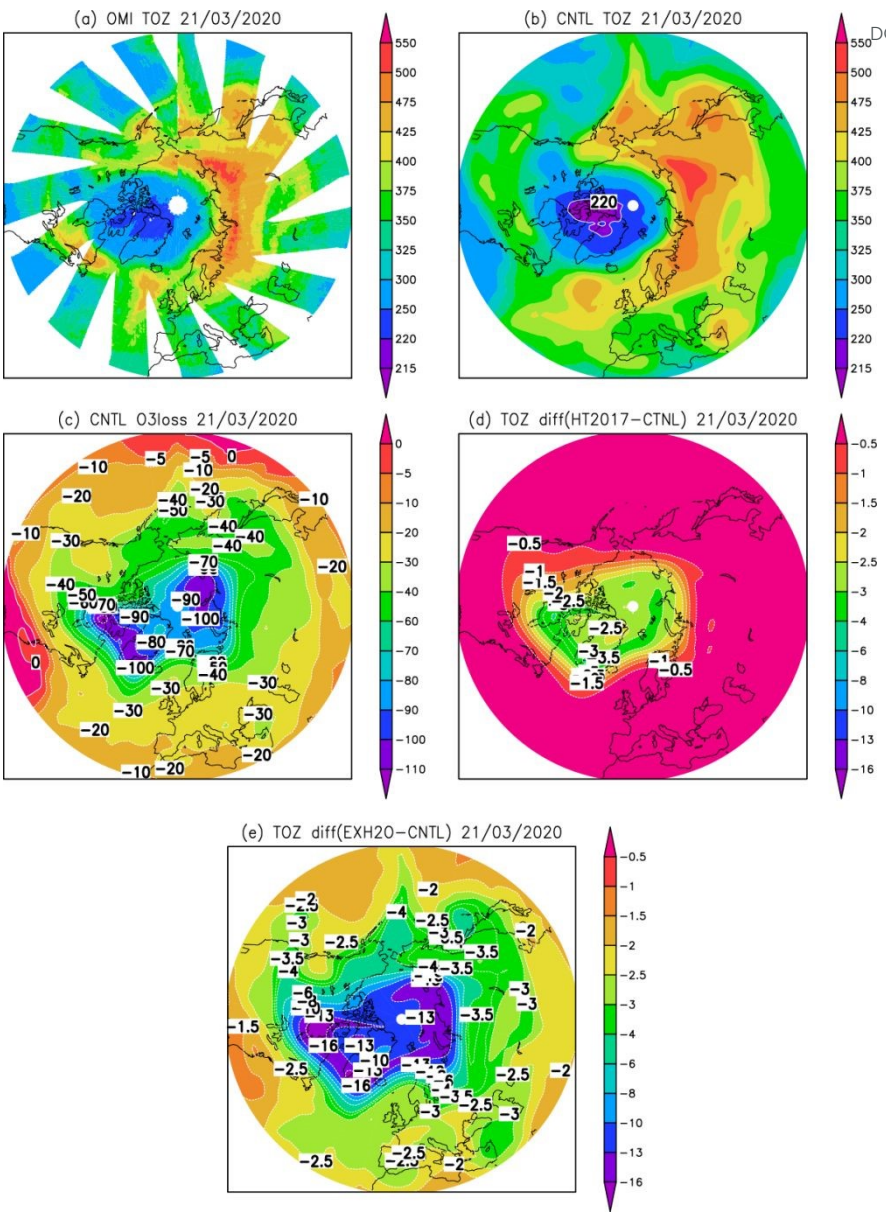

Figure 11. Total column ozone (DU) on March 21, 2020 (a) observed by OMI, (b) from model run CNTL, (c) chemical ozone loss (DU) from run CNTL (active minus passive), (d) difference in column ozone (DU) between run HT2017 and CNTL and (e) difference in column ozone (DU) between runs EXH2O and CNTL. In panels (a) and (b) the 220 DU contour is indicated in white.

View Article Online
DOI: 10.1039/D4FD00163J

Data Availability

Data availability. The OMI/OMPS data is available from https://ozonewatch.gsfc.nasa.gov/meteorology/figures/ozone

The MLS data is available from https://mls.jpl.nasa.gov/